ORIGINAL ARTICLE

JBMR®

Chronic Kidney Disease–Induced Vascular Calcification Impairs Bone Metabolism

Maria L Mace,[1] Eva Gravesen,[1] Anders Nordholm,[1,2] Soeren Egstrand,[1,2] Marya Morevati,[1] Carsten Nielsen,[3] Andreas Kjaer,[3] Geert Behets,[4] Patrick D'Haese,[4] Klaus Olgaard,[1] and Ewa Lewin[1,2]

[1]Department of Nephrology, Rigshospitalet, University of Copenhagen, Copenhagen, Denmark
[2]Department of Nephrology, Herlev Hospital, University of Copenhagen, Copenhagen, Denmark
[3]Department of Clinical Physiology, Nuclear Medicine and PET and Cluster for Molecular Imaging, Rigshospitalet, University of Copenhagen, Copenhagen, Denmark
[4]Department of Biomedical Sciences, Laboratory of Pathophysiology, University of Antwerp, Antwerp, Belgium

ABSTRACT

An association between lower bone mineral density (BMD) and presence of vascular calcification (VC) has been reported in several studies. Chronic kidney disease (CKD) causes detrimental disturbances in the mineral balance, bone turnover, and development of severe VC. Our group has previously demonstrated expression of Wnt inhibitors in calcified arteries of CKD rats. Therefore, we hypothesized that the CKD-induced VC via this pathway signals to bone and induces bone loss. To address this novel hypothesis, we developed a new animal model using isogenic aorta transplantation (ATx). Severely calcified aortas from uremic rats were transplanted into healthy rats (uremic ATx). Transplantation of normal aortas into healthy rats (normal ATx) and age-matched rats (control) served as control groups. Trabecular tissue mineral density, as measured by μCT, was significantly lower in uremic ATx rats compared with both control groups. Uremic ATx rats showed a significant upregulation of the mineralization inhibitors osteopontin and progressive ankylosis protein homolog in bone. In addition, we found significant changes in bone mRNA levels of several genes related to extracellular matrix, bone turnover, and Wnt signaling in uremic ATx rats, with no difference between normal ATx and control. The bone histomorphometry analysis showed significant lower osteoid area in uremic ATx compared with normal ATx along with a trend toward fewer osteoblasts as well as more osteoclasts in the erosion lacunae. Uremic ATx and normal ATx had similar trabecular number and thickness. The bone formation rate did not differ between the three groups. Plasma biochemistry, including sclerostin, kidney, and mineral parameters, were similar between all three groups. ex vivo cultures of aorta from uremic rats showed high secretion of the Wnt inhibitor sclerostin. In conclusion, the presence of VC lowers BMD, impairs bone metabolism, and affects several pathways in bone. The present results prove the existence of a vasculature to bone tissue cross-talk. © 2020 The Authors. *Journal of Bone and Mineral Research* published by Wiley Periodicals LLC on behalf of American Society for Bone and Mineral Research (ASBMR).

KEY WORDS: SYSTEMS BIOLOGY–BONE INTERACTORS; ANIMAL MODEL; WNT/β-CATENIN/LRPs; BONE HISTOMORPHOMETRY; BONE μCT

Introduction

A normal bone homeostasis seems to be essential for the maintenance of a healthy cardiovascular system. Several observational studies report an association between low bone mineral density (BMD) and the presence of vascular calcification (VC). This is found in aging, diabetes, chronic kidney disease (CKD), osteoporosis, and some rare bone diseases.[1–6] Not only is the inverse correlation between BMD and VC found in cross-sectional studies but also in longitudinal cohorts where progression of VC was accompanied with greater bone loss.[7–9] This suggests an interplay between the two pathological processes. The association has also been linked to clinical outcomes as the severity of osteoporosis is correlated to a higher risk of cardiovascular events.[10,11] Conversely, moderate aorta calcification has been linked to increased fracture risk.[12] The phenomenon is often referred to as the calcification paradox because of the divergent processes of bone demineralization and soft tissue mineralization.[13] Even though several lines of evidence demonstrate a concurrence of the pathological processes in the skeletal

Received in original form May 15, 2020; revised form October 21, 2020; accepted October 23, 2020.
Address correspondence to: Maria L Mace, MD, PhD, Department of Nephrology, Rigshospitalet, University of Copenhagen, 2730 Copenhagen, Denmark. E-mail: maria.lerche.mace@regionh.dk
Additional Supporting Information may be found in the online version of this article.
Journal of Bone and Mineral Research, Vol. 36, No. 3, March 2021, pp 510–522.
DOI: 10.1002/jbmr.4203

and cardiovascular system, the plausible mechanistic link between them is not well understood. It is widely thought that it is the bone disorder promoting the VC.[14]

The presence of disturbed bone turnover and development of soft tissue calcification is especially observed in CKD patients.[15] As kidney function declines, the patients develop severe disturbances in their mineral balance, namely phosphate retention, low calcium, and altered levels of αklotho, fibroblast growth factor 23 (FGF23), parathyroid hormone (PTH), and calcitriol. Consequently, kidney disease causes fragile bone and impairment of the bone's ability to buffer calcium and phosphate.[16–19] Even though many factors in the uremic condition stimulate the development and progression of VC, it is believed that the dysregulated mineral and bone metabolism has a fundamental role in the pathogenesis of VC in CKD.[20] Today these complications to kidney failure are classified as one syndrome named CKD mineral and bone disorder (CKD-MBD).[14] Classical treatment strategies for VC have limited effect in CKD patients and they have very high cardiovascular mortality.[21]

VC is classically divided into tunica intima calcification and tunica media calcification. Whereas tunica intima calcification is related to atherosclerosis with focal calcification of vascular plaques, tunica media calcification is a more generalized calcification of the medial layer of larger arteries. Media VC is found in aging, osteoporosis, diabetes, and especially pronounced in CKD. Even though both types of VC are found in CKD patients, the media VC is predominant.[22] Development of VC is a highly cell-regulated process, characterized by the phenotypic conversion of the vascular smooth muscle cell (VSMC) into a bone-like secretory cell. The differentiated VSMC expresses proteins of the osteoblastic lineage and secretes extracellular proteins in which hydroxyapatite crystals can precipitate.[23]

In a previous study from our lab, we used high-throughput RNA sequencing (RNA-seq) to characterize the transcriptional changes in the calcified aorta from 5/6 nephrectomized CKD rats.[24] Among the large changes in the transcriptome, in the 5/6 nephrectomized rats compared with rats with normal renal function, we found significant upregulation of the Wnt inhibitors sclerostin and secreted frizzled-related protein 4 (SFRP4). As both sclerostin and SFRP4 are circulating molecules, once secreted by the calcified vasculature, they could affect bone metabolism by inhibiting the anabolic Wnt pathway. As such, the general notion of impaired bone metabolism leading to VC may be too simple. We therefore propose a novel hypothesis that VC induces bone loss. To study the hypothesis, we developed a new model of isogenic aorta transplantation in inbred rats, in which the calcified abdominal aortas from 5/6 nephrectomized CKD rats are transplanted into healthy rats with normal renal function. The isogenic status of the rats has the added advantage in that transplantation can be performed without the use of immunosuppressive medication, which otherwise would affect bone turnover.[25,26] This new animal model thus enabled us to study the isolated effect of the presence of VC on bone in an otherwise healthy rat. Four weeks after the aorta transplantation, the bone's morphology, mineral density, and remodeling activity were examined. In addition, the aorta from normal and uremic rats was cultured ex vivo.

Materials and Methods

Animals

Inbred adult male dark agouti (DA) rats (7 weeks) (Envigo, Horst, The Netherlands) were used in the study. The genetic background of DA rat is characterized as isogenic. They were housed in an accredited facility with a 12-hour light/dark cycle and free access to food (Altromin 1324, Altromin Specialfutter, Lage, Germany) and water. The experiments were conducted in accordance to the national guidelines for care and use of laboratory animals. The experimental protocols were approved by the Danish Animal Experiments Inspectorate (license no. 2012-15-2934-00022).

Experimental protocol

1. Normal rats transplanted with a calcified aorta from 5/6 nephrectomized rats (uremic ATx) ($n = 16$)
2. Control group of normal rats transplanted with an aorta from rats with normal renal function and no VC (normal ATx) ($n = 10$)
3. Control group of age-matched rats with normal renal function (control) ($n = 6$)

Rats were randomized to experimental groups, yet a higher number of rats were allocated to the transplanted groups in case of postoperative complications.

Induction of vascular calcifications and chronic kidney disease (CKD) in the donor rat

Chronic uremia was induced by one-step 5/6 nephrectomy as previously described by our laboratory.[27] Rats were anesthetized with hypnorm-midazolam (Department of Experimental Medicine, University of Copenhagen, Copenhagen, Denmark). In a retroperitoneal approach, the right renal artery and vein were ligated and the kidney removed. The poles of the left kidney were removed, leaving 1/3 remnant of left kidney tissue. Rats were given carprofen (Rimadyl, Pfizer, Copenhagen, Denmark) subcutaneously as pain relief for the following 3 days. The induction of VC in the rat necessitates a high phosphate diet and treatment with an active vitamin D analog. To induce severe VC in the 5/6 nephrectomy model, the uremic rats were given a high-phosphate diet (0.9% calcium (Ca), 1.4% phosphate (P) and 600 IU cholecalciferol (vit D3) from Altromin (Altromin 1320 mod) starting 1 week after operation. After 8 weeks of uremia, rats were treated with 80 ng alfacalcidol (Leo Pharmaceutical, Copenhagen, Denmark) intraperitoneally 3 times weekly for 6 weeks. At the age of 22 weeks, after 14 weeks of uremia, severe VC has developed in the 5/6 nephrectomized rats, as previously published by our group.[24]

The novel model of isogenic uremic calcified aorta transplantation into a normal rat

A midline incision was placed in the linea alba and the intestines were gently moved to the right side in order to visualize the abdominal aorta. First, all side branches of the abdominal aorta were ligated with absorbable sutures. Then the abdominal aorta (20 mm in situ) was excised from the donor rat, flushed with heparin/saline, and immediately transplanted into a healthy recipient rat. Two microvascular clamps were placed on the abdominal aorta of the recipient, one distal to the iliolumbar arteries and one proximal to the aortic bifurcation. The recipient's aorta was incised right in between the two microvascular clamps and the graft was sutured with end-to-end anastomoses into the recipient's aorta (Supplemental Fig. S1). Exactly the same procedure was followed for transplantation of grafts from uremic rats and transplantation of grafts from normal rats. The aorta

transplantation was performed without use of immunosuppressive medication.[25,26] After the transplantation the uremic ATx, normal ATx and control rats were kept on a standard diet from Altromin (0.9% Ca, 0.7% P, and 600 IU vit D3) until euthanization after 4 weeks. No mortality was found in this model. However, in the present study, one normal ATx rat was euthanized 1 week after transplantation due to infection. This rat was excluded from the analyses.

Plasma biochemistry

Plasma levels of creatinine, urea, and phosphate were measured using a Vitros 250 analyzer (Ortho-Clinical Diagnostics, Raritan, NJ, USA). Ionized calcium was measured at actual pH by ABL 505 (Radiometer, Copenhagen, Denmark). Full-length fibroblast growth factor 23 (iFGF23) was measured using an intact FGF23 ELISA (Kainos Laboratory, Tokyo, Japan) with an intra-assay CV of 2.5% and interassay CV of 5% in our lab.[28] PTH was measured by a rat bioactive intact PTH ELISA (Immunotopics, San Clemente, CA, USA) with an intra-assay CV of 4% and an interassay CV of 9% in our lab.[29] Sclerostin levels in plasma and cell culture medium were measured using mouse/rat sclerostin ELISA (R&D Systems, Minneapolis, MN, USA) with an intra-assay CV of 3.5% in our lab.

Gene analysis by quantitative RT-PCR

The right femur was snap-frozen in liquid nitrogen after removal of soft tissue and the bone marrow. A specially designed mortar was placed shortly in liquid nitrogen and used to crush the bone. Total RNA was extracted using the EZNA RNA isolation kit (Omega Bio-tek, Norcross, GA, USA). Synthesis of cDNA was performed using the Superscript III cDNA kit (Invitrogen, Thermo Fischer Scientific, Waltham, MA, USA). Roche LightCycler 480 (Roche, Basel, Switzerland) with a temperature profile of 94°C for 2 minutes, 45 cycles of 94°C for 30 seconds, 59°C for 45 seconds, and 72°C for 90 seconds and JumpStart (Sigma-Aldrich, St. Louis, MO, USA) were used for quantitative real-time PCR. Melting curve analysis was performed to confirm a single PCR product. The mRNA levels were normalized to the mean of stabile reference genes *ARBP* and *RPL13*, and results are shown as the ratio to the expression levels of the control group. Reference gene stability was confirmed using geNorm.[30] Primers are listed in Supplemental Table S1.

Micro-computed tomography (μCT)

The left femur was dissected free from soft tissue, placed in 70% ethanol, and stored at 4°C. The whole femur was scanned with high-resolution μCT (Inveon μCT Scanner, Siemens, Munich, Germany). CT images were acquired with the following settings: 361 projections, 60 kV, 500 μA, and 1300 ms exposure. The CT images were reconstructed with a voxel size of 32 μm. Image analysis was performed using the Inveon Software (Siemens). The distal femur growth plate was used as reference (REF). The cortical bone cross-section area (Ct.Ar, mm^2) was measured 10 mm proximal to REF (Supplemental Fig. S2). For analysis of trabecular bone, a region of interest (ROI) of 0.960 mm along the longitudinal direction was drawn manually starting at 2.080 mm proximal to REF. The CT images of ROI were segmented into bone and marrow by a visually chosen fixed threshold for all groups. Bone morphometry was calculated using the Inveon Software (Siemens) based on the parallel plate model by Parfitt.[31] The following parameters were calculated: the ratio of total trabecular volume to total tissue volume (BV/TV), trabecular thickness (Tb.Th, mm), trabecular number (Tb.N, 1/mm), and trabecular spacing (Tb.Sp, mm). Tissue mineral density (TMD) was calculated by using phantom reference data. A standard bone phantom (Inveon, Siemens) was calibrated and applied to calculate the TMD of the trabecular bone (ROI). Results are expressed in milligrams/cubic centimeter (mg/cc).

Bone histomorphometry

The method for quantitative histomorphometry of bone has been described elsewhere.[32] Briefly, left tibias were fixed in ethanol 70% and subsequently dehydrated and embedded in a methylmethacrylate resin. Undecalcified 5-μm-thick sections were stained by the method of Goldner for quantitative histology to determine static bone parameters. Sections (10 μm thick) were mounted unstained in 100% glycerol for fluorescence microscopy and visualization of tetracycline and demeclocycline labels to determine dynamic bone parameters. All rats had intraperitoneal injections of 30 mg/kg tetracycline and 25 mg/kg demeclocycline, respectively, 7 and 3 days before euthanization. Results are reported as measurements in two dimensions using nomenclature established by the American Society for Bone and Mineral Research.[33] Bone analysis was performed on the bone tissue, one microscopic field from proximal growth plate and cortical bone (200× magnification, Supplemental Fig. S3), using a semi-automatic image analysis program (AxioVision v 4.51, Zeiss, Jena, Germany) running a custom program. Key parameters that were assessed included mineral apposition rate (MAR, μm/d), bone formation rate on bone surface (BFR/BS, $\mu m^2/mm^2/d$), mineralizing surface (MS/BS, %), mineralization lag time (MLT, days), adjusted apposition rate (Aj.AR, μm/d), perimeter of active osteoblasts on total perimeter (Ob.Pm/Tt.Pm, %), perimeter of active osteoclasts on total perimeter (Oc.Pm/Tt.Pm, %), eroded perimeter on total perimeter (E.Pm/Tt.Pm, %), tetracycline- and demeclocycline-labeled bone perimeter on bone perimeter (dL.Pm/B.Pm), bone area on tissue area (B.Ar/T.Ar, %), Tb.N (N/mm), Tb.Th (μm), Tb.Sp (μm), osteoid area on bone area (O.Ar/B.Ar, %), osteoid perimeter on total perimeter (O.Pm/Tt.Pm, %), and osteoid width (μm).

Aorta culture

The aortas from two normal rats and three uremic rats were cultured ex vivo. Under sterile conditions, the whole aorta was gently excised (from arcus aorta to aortic bifurcation) under a stereomicroscope. The vessel was flushed with heparin/saline and placed in cold isotonic saline. While suspended in saline, the aorta was gently cut into 1-mm pieces under a stereomicroscope. The aorta rings were then quickly placed in Dulbecco modified Eagle's medium (DMEM) high glucose (D5796, Sigma-Aldrich) supplemented with 10% fetal bovine serum (heat inactivated, 30–2025, ATCC, Feddington, UK) and 1% penicillin/streptomycin. Eight aorta rings were placed per well in a 12-well cell plate (polystyrene, nunclon delta surface, Thermo Fisher Scientific), suspended in 1 mL complete media and incubated at 37°C in a 5% CO_2 atmosphere. The culture time was either 24 or 48 hours, after which the media was collected and its concentration of sclerostin was measured using mouse/rat sclerostin ELISA (R&D Systems). We also measured the complete media without aorta rings (sole media) at the same time points. Viability of the aorta rings was confirmed by Trypan blue staining (data not shown).

Statistics

Normal distributed data are expressed as mean ± SD. Skewed data are shown as median [range]. Data are presented in box plots showing median, interquartile range, and all data points in all figures. Statistical significance was tested using two-sided *t* test for data with normal distribution and the Mann–Whitney *U* test as nonparametric test. One-way ANOVA followed by Tukey's multiple-comparison tests was used to compare means between the three groups. Calculated in Prism 8.0 or Excel 2016. Significance level was set at $p < .05$.

Results

Donor rats

The uremic donor rats suffered from severe kidney failure with doubled creatinine levels and disturbed mineral metabolism compared with the normal donor rat (Supplemental Table S2). At the time of transplantation, the normal donor aorta graft contained no calcium, whereas the aorta graft from uremic rats had a high calcium content of 15.7 ± 3.2 μg/mg dry weight as published elsewhere.[34] The normal and calcified aortas' expression levels of genes involved in Wnt signaling are shown in Supplemental Table S3. The severe VC was associated with the development of renal osteodystrophy, as all the uremic rats had abnormal bone (Supplemental Figs. S4 and S5). Also, the uremic rats had significantly higher plasma levels of sclerostin 768 ± 137 pg/mL versus the normal donor rats 110 ± 20 pg/mL, $p < .001$ (Supplemental Table S2). In bone, however, the mRNA levels of sclerostin were downregulated by one-third in the uremic rats compared with normal rats (Supplemental Fig. S6).

Plasma biochemistry

All recipient rats were euthanized 4 weeks after transplantation and blood was drawn for measurement of biochemical parameters of kidney function and mineral homeostasis. The plasma biochemistry of control, normal ATx, and uremic ATx rats is shown in Table 1. All rats had normal kidney function and there was no difference in plasma creatinine (Table 1) and urea (data not shown) levels between groups. All rats had similar levels of ionized calcium, PTH, and FGF23. The normal ATx group had slightly but significantly ($p = .003$) lower levels of phosphate in comparison to uremic ATx; however, no difference was found between control and uremic ATx.

We previously demonstrated that the Wnt inhibitor sclerostin is in the top 10 most upregulated genes in the calcified aorta in this model (Supplemental Table S3).[24] To examine if this signal molecule was leaked to the bloodstream by the calcified aorta graft, we measured the plasma levels of sclerostin at euthanization in all three groups but found similar levels ($p = .082$) (Table 1).

Bone morphology and tissue mineral density measured by μCT

We performed μCT of the femur bone ex vivo. Trabecular TMD was significantly lower in the uremic ATx rats compared with normal ATx rats (1576 ± 19 versus 1592 ± 16 mg/cc, $p = .045$). Control rats had a TMD of 1613 ± 15 mg/cc, which was significantly higher than the ones measured in both groups of transplanted rats (control versus normal ATx, $p = .023$, and control versus uremic ATx, $p < .001$, Fig. 1*A*). Bone volume was also slightly higher in control rats with increased trabecular thickness compared with both transplanted groups (Table 2). No difference in cancellous bone parameters was found between normal ATx and uremic ATx as well as in the cortical cross-section area (Table 2 and Fig. 1*D*).

Bone formation and mineralization

To further study the effect of the presence of a severely calcified aorta on bone mineralization, we measured mRNA levels of genes coding for proteins involved in extracellular matrix and bone mineralization by qPCR. A doubling of mRNA levels of the mineralization inhibitor osteopontin was found in the bone of uremic ATx rats compared with normal ATx and control rats (2.98 ± 1.47 versus 1.40 ± 1.04 and 1.0 ± 0.30, $p = .002$ and $p < .001$, respectively, Fig. 2*A*). We also found a large increase in progressive ankylosis protein homolog (ANKH), which inhibits mineralization through regulation of pyrophosphate levels. More specifically, ANKH mRNA levels in uremic ATx rats were 3.38 ± 1.00 versus normal ATx rats 1.34 ± 0.93 and control 1.0 ± 0.49, both $p < .001$ (Fig. 2*B*). Alkaline phosphatase mRNA levels were also significantly higher in uremic ATx rats compared with normal ATx and control rats (3.81 ± 1.38 versus 1.83 ± 1.13 and 1.0 ± 0.35, both $p < .001$, Fig. 2*C*). In addition, the most abundant extracellular protein in bone collagen I was also more expressed in the uremic ATx rats compared with normal ATx and control rats (median 2.86 [0.84; 4.55] versus 0.71 [0.1; 5.94] and 1.0 [0.5; 2.31], $p = .003$ and $p = .001$, respectively, Fig. 2*D*). There was no difference in mRNA levels in all four genes between control groups of normal ATx and control rats. Furthermore, there was no difference in FGF23 mRNA levels in all three groups (Supplemental Fig. S7).

Altered bone turnover markers in rats transplanted with a uremic calcified aorta

We also explored whether there was an effect of VC on bone turnover by measuring the mRNA levels of genes coding for proteins, which are commonly used as bone turnover markers. We found a downregulation of the osteoblast-derived osteocalcin indicating an impaired bone formation in uremic ATx rats. Osteocalcin mRNA levels were reduced by one-half in uremic ATx

Table 1. Plasma Biochemistry

Group	Creatinine (μM)	Ca^{2+} (mM)	Phosphate (mM)	PTH (pg/mL)	iFGF23 (pg/mL)	Sclerostin (pg/mL)
Control	34 ± 8	1.28 ± 0.02	1.21 ± 0.31	27 [12; 194]	223 ± 60	186 ± 50
Normal ATx	29 ± 4	1.27 ± 0.04	0.99 ± 0.21[a]	30 [1; 140]	187 ± 43	137 ± 43
Uremic ATx	30 ± 3	1.29 ± 0.03	1.33 ± 0.26	32 [12; 2392]	205 ± 60	151 ± 34

PTH = parathyroid hormone; iFGF23 = intact fibroblast growth factor 23; ATx = isogenic aorta transplantation.

Similar plasma biochemistry was found in all groups excluding phosphate levels in normal ATx(a), which was similar to control ($p = .12$) but significantly lower to uremic ATx ($p = .003$). There was no difference in plasma levels of phosphate between uremic ATx and control ($p = .36$). Data are shown as mean ± SD except PTH, which is expressed as median [range]. Control $n = 6$, normal ATx $n = 9$, uremic ATx $n = 16$.

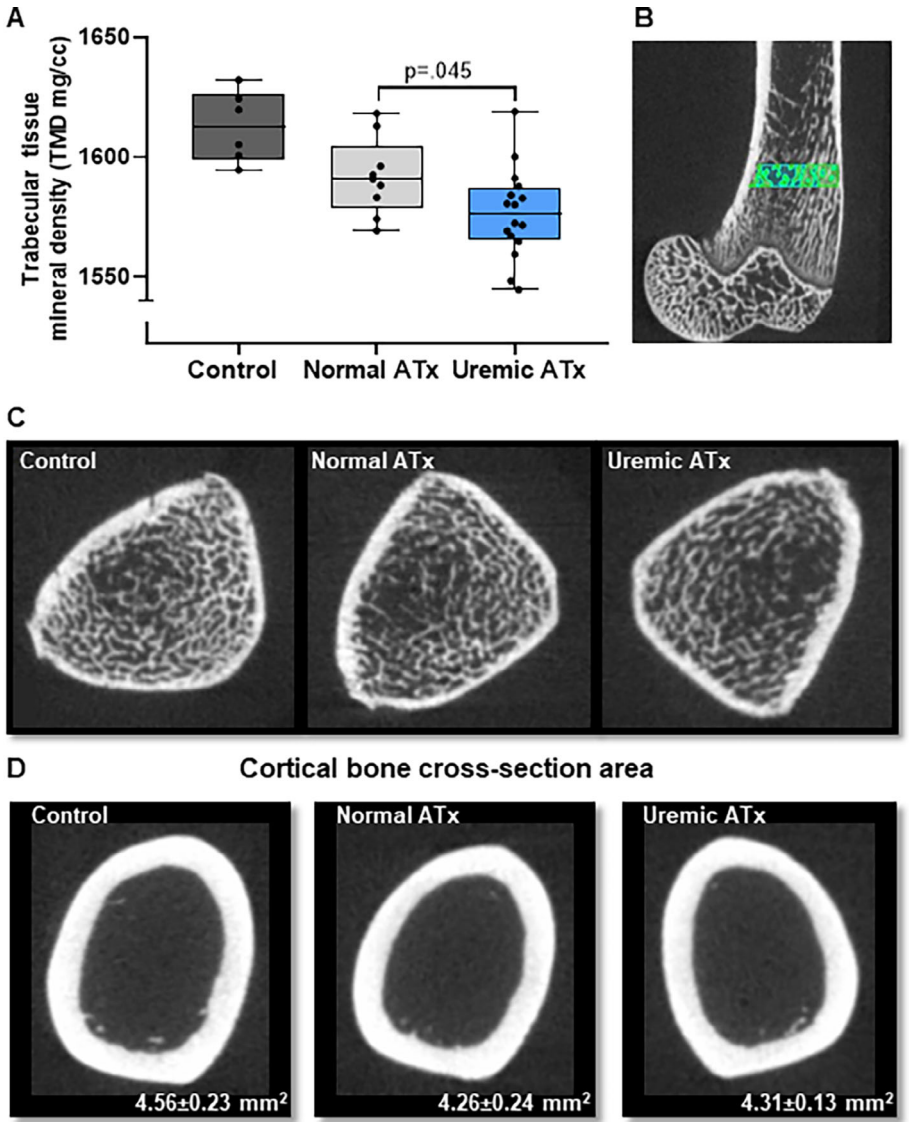

Fig 1. Micro-computed tomography (μCT) analysis of femur bone. (*A*) Tissue mineral density (TMD) of the trabecular bone. Significantly lower TMD was found in rats transplanted with a calcified aorta from uremic rats (uremic ATx) compared with rats transplanted with a normal aorta (normal ATx), $p = .045$. Control rats had higher TMD compared with both transplanted groups versus normal ATx, $p = .023$, and versus uremic ATx, $p < .001$. (*B*) Illustration of the analyzed area of the trabecular bone (the region of interest [ROI]). (*C*) μCT imaging of the cross section of bone in all three groups at proximal ROI. (*D*) μCT image of the cortical bone cross-section area (Ct.Ar). Slightly higher Ct.Ar was found in controls compared with transplanted rats ($p = .014$). No difference was found between normal ATx and uremic ATx. Data are shown as box plots with median, interquartile range, and all data points in *A* and mean ± SD in *D*. Control $n = 6$, normal ATx $n = 9$, uremic ATx $n = 16$.

Table 2. Bone Morphology Measured by μCT

Group	BV/TV (ratio)	Tb.N (1/mm)	Tb.Th (mm)	Tb.Sp (mm)	Ct.Ar (mm^2)
Control	0.65 ± 0.08	5.03 ± 0.35	0.13 ± 0.02	0.07 ± 0.01	4.56 ± 0.23
Normal ATx	0.52 ± 0.10	5.07 ± 0.35	0.10 ± 0.02	0.10 ± 0.03	4.26 ± 0.24
Uremic ATx	0.54 ± 0.08	5.23 ± 0.19	0.10 ± 0.01	0.09 ± 0.02	4.31 ± 0.13

BV/TV = trabecular bone volume/tissue volume; Tb.N = trabecular number; Tb.Th = trabecular thickness; Tb.Sp = trabecular spacing; Ct.Ar = cortical bone cross-section area; ATx = isogenic aorta transplantation.

Both transplanted groups had significantly lower BV/TV with decreased Tb.Th and increased Tb.Sp compared with control ($p = .025$, $p = .005$, $p = .028$, respectively). No difference was found between normal ATx and uremic ATx. Tb.N was the same in all groups. Also, the Ct.Ar was smaller in the transplanted rats compared with control ($p = .020$), but no difference was found between normal ATx and uremic ATx. Data are expressed as mean ± SD. Control $n = 6$, normal ATx $n = 9$, uremic ATx $n = 16$.

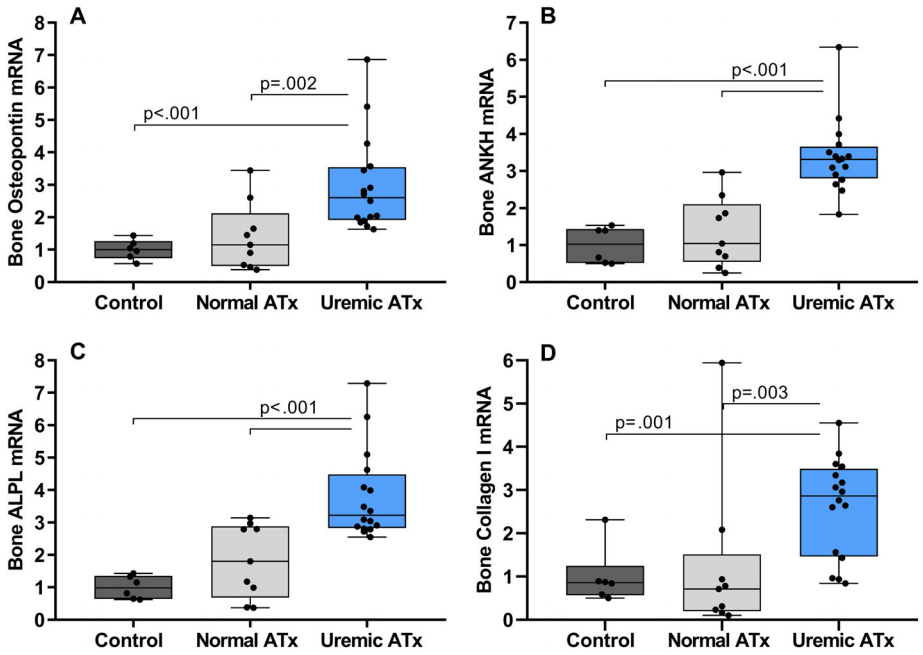

Fig 2. Bone expression of genes involved in bone mineralization and formation. (*A–D*) Rats transplanted with a calcified aorta from uremic rats (uremic ATx) had significantly increased mRNA levels of osteopontin (*A*), progressive ankylosis protein homolog (ANKH) (*B*), alkaline phosphatase (ALPL) (*C*), and collagen type I α2 (collagen I) (*D*) compared with rats transplanted with a normal aorta (normal ATx) and control rats. There was no difference in the expression of these genes between normal ATx and control. The mRNA levels of genes are normalized to reference genes Arbp and Rpl13 and shown as the ratio to the mean of control group. Data are shown as box plots with median, interquartile range, and all data points. Control $n = 6$, normal ATx $n = 9$, uremic ATx $n = 16$.

0.46 ± 0.21 versus normal ATx 0.77 ± 0.36, $p = .047$, uremic ATx versus control 1.0 ± 0.12, $p < .001$. There was no difference between normal ATx and control (Fig. 3*A*). Inversely, the osteoclast-derived cathepsin K was significantly upregulated in uremic ATx rats, indicating increased bone resorption. More specifically, uremic ATx 2.32 ± 0.96 versus normal ATx 1.17 ± 0.67 and control 1.0 ± 0.17, $p = .002$ and $p < .001$, respectively (Fig. 3*B*). The communication between osteocyte/osteoblast–osteoclast was also affected by the presence of the calcified aorta graft as indicated by a strong downregulation of the receptor activator of nuclear factor kappa-B ligand (RANKL) expression in uremic ATx rats (uremic ATx 0.17 ± 0.09 versus normal ATx 0.79 ± 0.44, $p = .003$ and uremic ATx versus control 1.0 ± 0.30, $p < .001$, Fig. 3*C*). The key osteoblast transcription factor Runt-related transcription factor 2 (RUNX2) was upregulated in uremic ATx 2.86 ± 0.64 compared with normal ATx 1.51 ± 1.04 and control 1.0 ± 0.33, $p = .005$ and $p < .001$, respectively (Fig. 3*D*). Normal ATx and control had similar mRNA levels in all of the above-mentioned genes.

Disturbed expression of genes involved in Wnt signaling in bone

The canonical Wnt/β-catenin signaling is an important bone formation regulatory pathway in normal bone homeostasis. The osteocytes express and secrete sclerostin, a powerful Wnt inhibitor that exerts anti-anabolic effects on bone.[35] We found a large upregulation of sclerostin in bone from uremic ATx rats compared with normal ATx and control rats (median: 2.80 [1.48; 12.80] versus 1.18 [0.31; 3.08] and 1.0 [0.38; 2.11], both $p < .001$, Fig. 3*E*).

Bone morphogenetic protein 2 (BMP2) is an important stimulator of bone formation. Its expression was slightly but significantly downregulated in uremic ATx rats, whereas the same mRNA levels were found in normal ATX and control rats (0.80 ± 0.15 versus 1.02 ± 0.22 and 1.0 ± 0.27, $p = .021$ and $p = .035$, respectively, Fig. 3*F*).

The calcified aorta expresses the Wnt inhibitors sclerostin and SFRPs.[24] If these signaling molecules are secreted into circulation, they could exert an endocrine function on bone. Therefore, we examined the activity of Wnt signaling in bone by measuring the expression level of β-catenin in the canonical Wnt pathway. We found an upregulation of β-catenin mRNA levels in uremic ATx rats 3.07 ± 0.98 compared with normal ATx 1.25 ± 0.76 and control 1.0 ± 0.31, both $p < .001$ (Fig. 4*A*). Activation of the Wnt pathway in bone upregulates c-Myc and Axin2.[36] In the uremic ATx rats, c-Myc mRNA levels were lower in comparison to normal ATx (0.69 ± 0.28 versus 1.20 ± 0.68, $p = .037$) and control (0.69 ± 0.28 versus 1.0 ± 0.22, $p = .031$, Fig. 4*B*). Also, Axin2 mRNA was downregulated in uremic ATx rats versus normal ATx rats (0.97 ± 0.55 versus 1.48 ± 0.56, $p = .038$) but similar to control rats (0.97 ± 0.55 versus 1.0 ± 0.22, $p = .79$, Fig. 4*C*). Cyclin D1 is one of the target genes of the canonical Wnt signaling pathway.[36] Control rats had a variation in the mRNA expression level of this gene with no difference found between the groups (control 1.2 ± 0.68, normal ATx 1.38 ± 0.28, uremic ATx 1.49 ± 0.69, $p = .59$, Fig. 4*D*). The canonical and non-canonical Wnt signaling regulates the expression of Snail1, which was significantly upregulated in uremic ATx rats 3.60 ± 1.29 versus

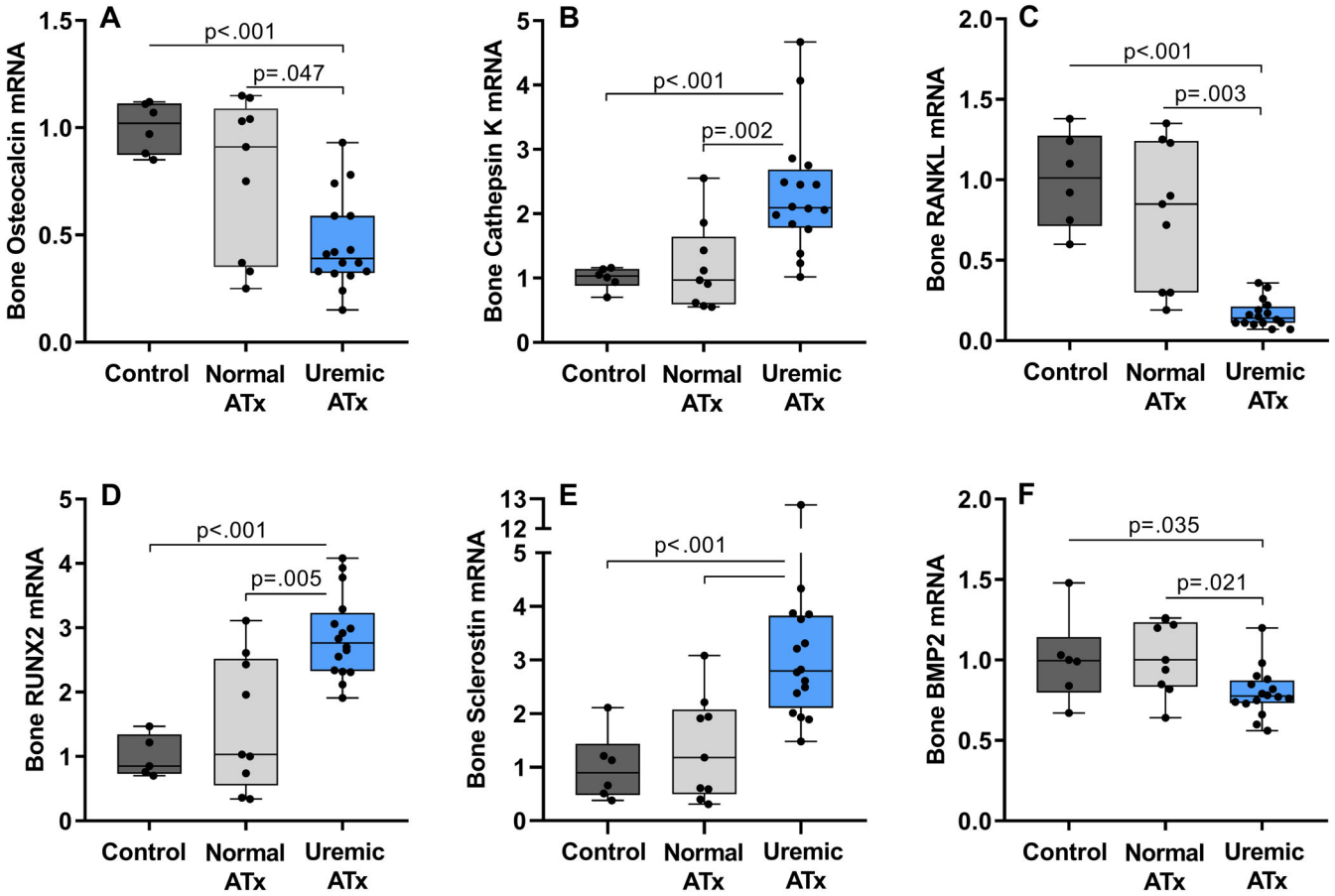

Fig 3. Bone expression of genes related to bone turnover. (*A*, *C*, *F*) Rats transplanted with a calcified aorta from uremic rats (uremic ATx) had significantly decreased mRNA levels of osteocalcin (*A*), receptor activator of nuclear factor kappa-B ligand (RANKL) (*C*), and bone morphogenetic protein 2 (BMP2) (*F*) compared with rats transplanted with a normal aorta (normal ATx) and control rats. (*B*, *D*, *E*) Cathepsin K (*B*), runt-related transcription factor 2 (RUNX2) (*D*), and sclerostin (*E*) were significantly upregulated in uremic ATx compared with both control groups. No difference in mRNA levels were found between normal ATx and control. The mRNA levels of genes are normalized to reference genes Arbp and Rpl13 and shown as the ratio to the mean of control group. Data are shown as box plots with median, interquartile range, and all data points. Control $n = 6$, normal ATx $n = 9$, uremic ATx $n = 16$.

normal ATx 1.48 $\pm$ 1.30 and control 1.0 $\pm$ 0.29, both $p < .001$, Fig. 4*E*).

Analysis of static and dynamic bone parameters by bone histomorphometry

We further analyzed bone by performing quantitative bone histomorphometric analysis on sections of the tibia. In the histological sections, we measured a series of static and dynamic bone parameters. Similar to the findings by μCT, both groups of transplanted rats had slightly lower bone area compared with control rats (28.5 $\pm$ 3.4%). There was no difference in bone area between uremic ATx and normal ATx (23.1 $\pm$ 4.6% versus 22.1 $\pm$ 4.7%, Fig. 5*A*), with same trabecular number and thickness (Supplemental Fig. S8). Remarkably, there was significantly lower osteoid area in the uremic ATx rats compared with normal ATx rats (median 0.3% [0.03; 0.8] versus 0.5% [0.2; 0.8], $p = .036$, Fig. 5*B*). A representative histological image is shown in Fig. 5*G*. Same osteoid width was found in all three groups (Fig. 5*C*). There was no difference in the mineralizing surface between the three groups. Also, bone formation rate did not differ between groups (Fig. 5*D*, *E*). However, there was a distinct trend toward an increased adjusted apposition rate in the uremic ATx group versus normal ATx and control groups, which, however, did not reach statistical significance due to the large biological variability within the uremic ATx group (Fig. 5*F*). Mineral apposition rate is shown in Supplemental Fig. S8.

The osteoid perimeter was lower in uremic ATx rats compared with normal ATx rats (Fig. 6*A*). Although not statistically significant, a higher number of rats in the uremic ATx group relative to the total number (8/16; 50%) in this group did not show active osteoblasts lining the osteoid seam compared with the normal ATx group (1/9; 11%) (Figs. 5*G* and 6*B*). On the other hand, only 6 of 16 rats (38%) of the uremic ATx group showed empty erosion lacunae; ie, no osteoclasts compared with 6 of 9 (67%) in the normal ATx group (Fig. 6*D* and representative images, Fig. 6*E*). The eroded perimeter was similar among all three groups (Fig. 6*C*).

In vitro study

To examine if sclerostin was secreted by the vasculature, the aorta from normal and uremic rats were cultured ex vivo for 24 or 48 hours, and the media's concentration of sclerostin was

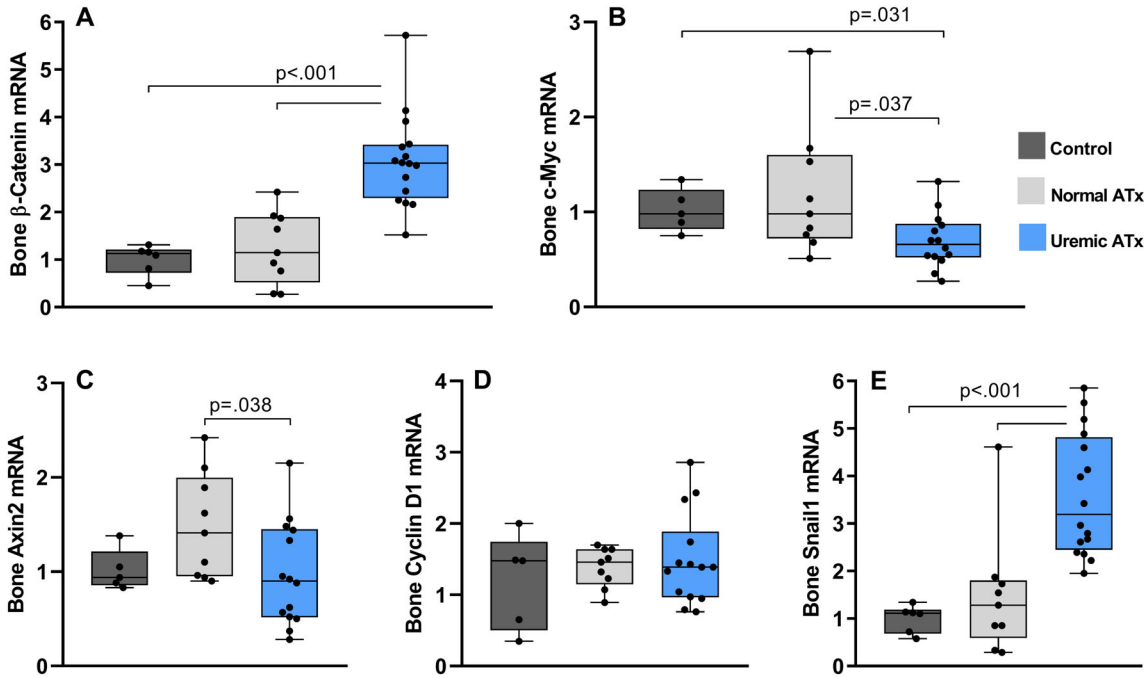

Fig 4. Bone expression of genes involved in Wnt signaling in bone. (*A*) β-catenin was significantly upregulated in rats transplanted with a calcified aorta from uremic rats (uremic ATx) compared with rats transplanted with a normal aorta (normal ATx) and control rats. (*B*) The mRNA levels of c-Myc were significantly downregulated in uremic AT compared with normal ATx and control. (*C*) Axin2 mRNA was also downregulated in uremic ATx compared with normal ATx but similar expression to control. (*D*) There was no difference in the mRNA levels of cyclin D1 between the three groups. (*E*) The mRNA levels of Snail1 were significantly increased in uremic ATx compared with normal ATx and control. No difference was found in the mRNA levels of all five genes between normal ATx and control. The mRNA levels of genes are normalized to reference genes Arbp and Rpl13 and shown as the ratio to the mean of control group. Data are shown as box plots with median, interquartile range, and all data points. Control $n = 6$ (5 in *B–D*), normal ATx $n = 9$, uremic ATx $n = 16$ (14 in *B–D*).

measured. Sclerostin could not be detected in the media without aorta rings (sole media). Small amounts of sclerostin were measured in the media with normal aorta rings that is 51 ± 26 pg/mL at 24 hours and 31 ± 9 pg/mL at 48 hours. In contrast, significantly higher concentrations were found in the media with uremic aorta rings, more specifically 1706 ± 883 pg/mL at 24 hours and 2367 ± 1463 pg/mL at 48 hours, compared with normal aorta incubation $p = .006$ (Fig. 7).

Discussion

The presence of VC, disturbed bone metabolism, and decreased BMD coincide in many different medical conditions, the so-called calcification paradox. The observations indicate a possible existence of an interplay between the skeletal and cardiovascular system. Our group has previously demonstrated a pronounced upregulation of Wnt inhibitors in the calcified aorta from CKD rats.[24,37] Therefore, the question was raised to which extent the development and presence of VC also affects bone tissue, thereby linking the dysfunction of the two tissues in a pathological cross-talk. To address this interesting research question, we developed a new animal model for studying the isolated effect of VC on bone: the isogenic aorta transplantation (ATx) model. We found significantly lower trabecular TMD in uremic ATx compared with control groups of normal ATx and control rats, indicating that the presence of VC alters the mineralization process in bone. In addition, we found significant upregulation of the mineralization inhibitors osteopontin and ANKH in the bone of the uremic ATx rats. Gene analyses of bone furthermore pointed toward a lower bone formation, higher bone resorption, altered osteoblast differentiation, and impaired osteoblast/osteocyte–osteoclast communication in the uremic ATx rats compared with normal ATx and control rats. In line herewith, in the bone histomorphometry analysis we found less osteoid, a trend toward fewer osteoblasts, and more osteoclasts in the uremic ATx rats compared with normal ATx rats. The bone formation rate, however, did not differ between groups. ex vivo cultures of aorta rings from normal and uremic rats showed a high secretion of sclerostin form the uremic calcified aorta. These novel findings support a direct effect of VC on bone metabolism.

We previously reported that the increased calcium content in the calcified aorta graft is not reversed when transplanted into a healthy recipient, and no calcification develops in the normal graft during the 4 weeks of implantation.[34] Rats transplanted with a uremic calcified graft had a lower trabecular TMD compared with rats transplanted with normal grafts without calcifications as well as compared with age-matched control rats. Several epidemiological studies have focused on the concomitant occurrence of VC and bone loss.[1,7–9,38] In all of these studies, however, it was assumed that VC developed as a result of disturbed bone metabolism. Our results expand the clinical observations, illustrating a direct effect of the presence of VC on bone metabolism and identify sclerostin as one of the secreted factors from

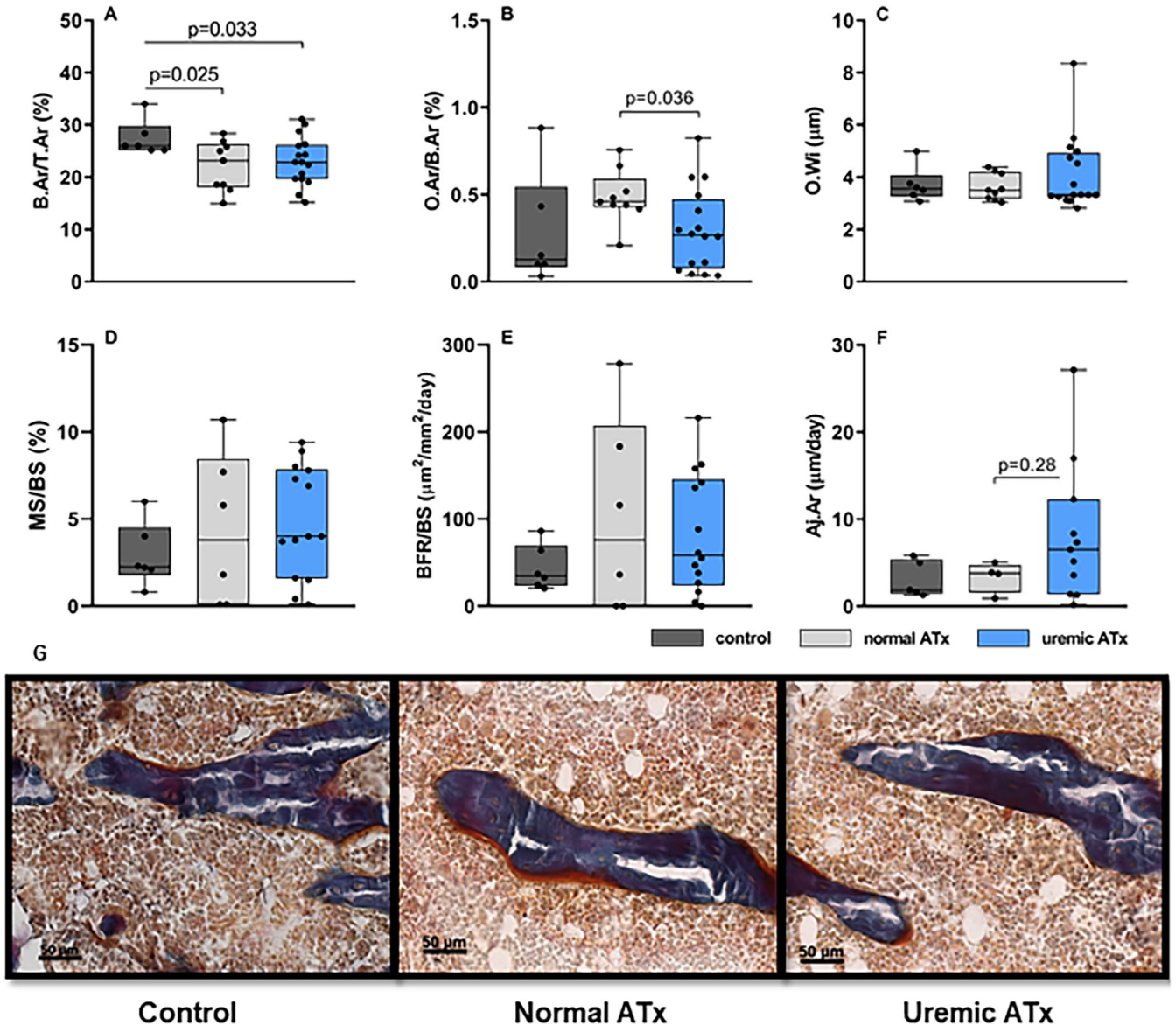

Fig 5. Bone histomorphometry analysis of static and dynamic bone parameters. (*A*) No difference in bone area (B.Ar/T.Ar, %) between rats transplanted with a calcified aorta from uremic rats (uremic ATx) compared with rats transplanted with a normal aorta (normal ATx). Bone area was slightly higher in control. (*B*) There was significantly lower osteoid area (O.Ar/B.Ar,%) in uremic ATx compared with normal ATx, with no difference with control. (*C*) Same osteoid width (O.Wi) among all three groups. (*D*) No difference in mineralizing surface (MS/BS, %) between all three groups. (*E*) Similar bone formation rate (BFR/BS, $\mu m^2/mm^2/d$) was found in all three groups. (*F*) The adjusted apposition rate (Aj.AR), which represents the bone formation rate averaged over the entire osteoid surface, showed a trend toward an increase in uremic ATx rats. Still, not statistically significant. (*G*) Representative Goldner-stained section of tibia bone, illustrating the osteoid (orange) and osteoblasts. Data are shown as box plots with median, interquartile range, and all data points. Control $n = 6$, normal ATx $n = 9$, uremic ATx $n = 16$. Due to technical error (poor uptake/one label) with tetracycline/demeclocycline, calculation of BFR is missing in 5 rats.

the calcified vasculature. The TMD of the normal ATx rats was slightly lower than control rats, which most likely is due to the surgical procedure. Both control groups were used in the study to assess the effect of the transplantation on bone by itself.

Our findings showing an effect of VC on bone formation and mineralization are supported by a recent study in rats with warfarin-induced VC.[39] Warfarin inhibits the production of biological active matrix γ-carboxyglutamic acid protein (MGP), which is a local inhibitor of VC in the vasculature. In the bone histomorphometric analysis, De Maré and colleagues found that warfarin-treated rats had mildly lower bone area and mineralized area compared with control rats without warfarin treatment.[39] Similar to our results, they found a trend toward less osteoid and reduced number of osteoblasts in rats with warfarin-induced VC, whereas the bone formation rate did not differ from controls.[39] BMD was not measured in the study.

Transplantation of small sections of calcified aortas has previously been performed in mice lacking the transmembrane

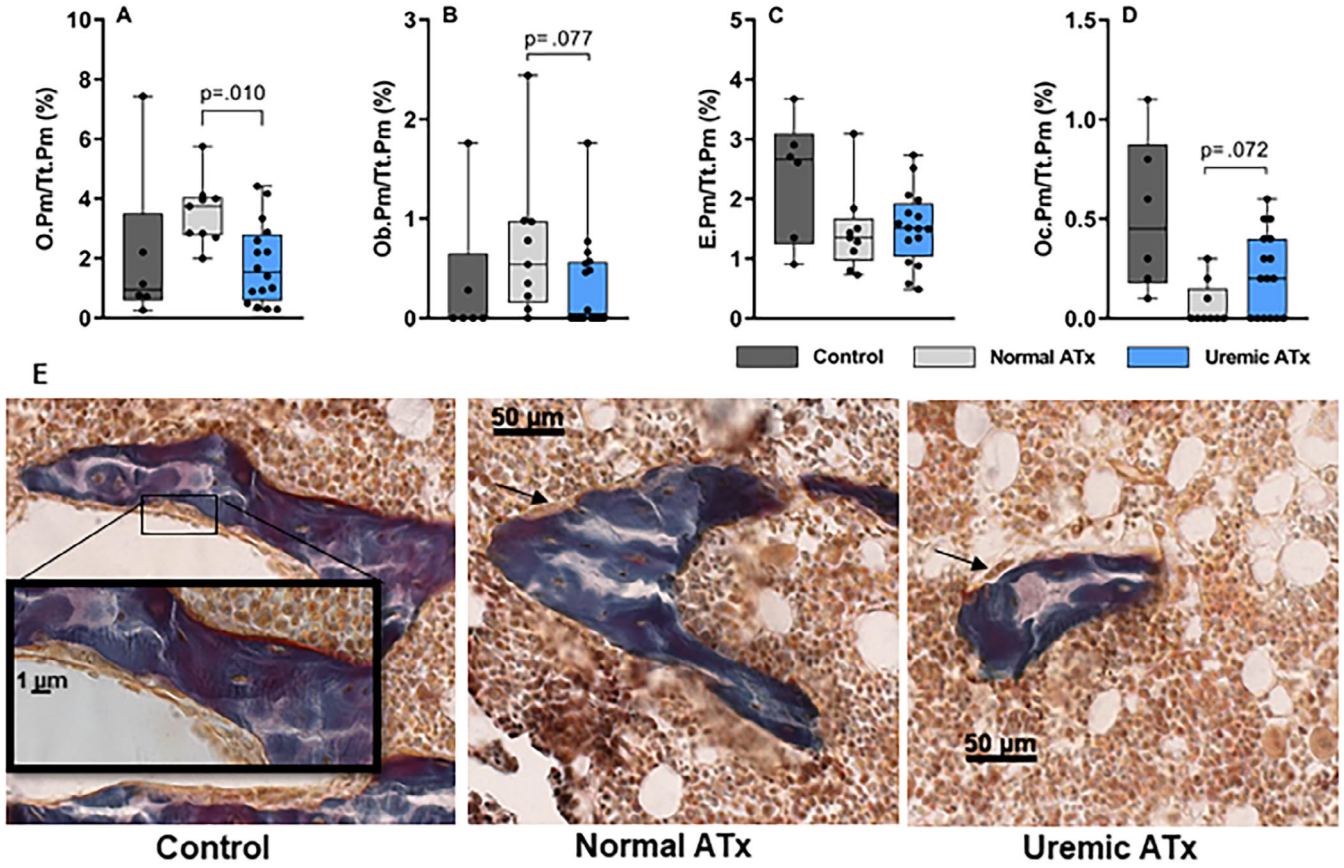

Fig 6. Bone histomorphometry analysis. (*A*) Rats transplanted with a calcified aorta from uremic rats (uremic ATx) had less osteoid perimeter on total perimeter (O.Pm/Tt.Pm%) compared with rats transplanted with a normal aorta (normal ATx), yet no difference with control. (*B*) Perimeter of active osteoblasts on total perimeter (Ob.Pm/Tt.Pm, %). There was a nonsignificant trend toward fewer osteoblasts in the uremic ATx rats. (*C*) Similar eroded perimeter on total perimeter (E.Pm/Tt.Pm, %) in all three groups. (*D*) Perimeter of active osteoclasts on total perimeter (Oc.Pm/Tt.Pm, %). The uremic ATx rats tended to have more osteoclasts, yet not statistically significant. (*E*) Representative Goldner-stained section of tibia bone, illustrating erosion surface and osteoclasts. Control: enlarged section of bone erosion surface visualizing osteoclasts. Normal ATx: black arrow marks the eroded surface without osteoclasts. Uremic ATx: black arrow points at osteoclast present in the resorption area. Data are shown as box plots with median, interquartile range, and all data points. Control $n = 6$, normal ATx $n = 9$, uremic ATx $n = 16$.

protein ectonucleotide pyrophosphatase phosphodiesterase (Enpp1), which produces pyrophosphate (PPi). In accordance to our previous findings, the established VC was not reversed by transplantation into a healthy recipient. Bone was not examined in the latter study.[40]

The bone remodeling cycle is a complex process of bone resorption, formation, and mineralization of newly formed osteoid. Even though key functions of the osteoblast, osteoclast, and osteocyte in bone turnover have been identified, the molecular biology of the process is only sparsely understood. The same accounts for the initiation and regulation of hydroxyapatite deposition and propagation in the mineralization process.[41] The pleiotropic glycoprotein osteopontin is a negatively charged bone matrix protein, which, among its multiple functions, has the ability to bind calcium with a high affinity.[42] In this way, it is thought that osteopontin inhibits crystal growth.[43] Higher plasma levels of osteopontin have been linked to lower BMD in cohort studies.[44,45] This is in line with our findings showing a significant upregulation of osteopontin mRNA levels in bone, thus providing one possible explanation to the impaired mineralization in the uremic ATx rats.

We also found a significant increase in ANKH, which is a transmembrane protein that transports inorganic pyrophosphate (PPi). PPi is a strong inhibitor of hydroxyapatite mineralization.[46] The upregulation of ANKH may result in a marked increase in PPi, which in turn will inhibit the mineralization process. However, its upregulation occurred together with an increase in alkaline phosphatase mRNA. Alkaline phosphatase hydrolyzes PPi to generate inorganic phosphate (Pi), an important substrate for hydroxyapatite generation and growth.[41] Since both ANKH and alkaline phosphatase increased in the uremic ATx, it is difficult to estimate the resulting changes in the PPi/Pi ratio. In bone, the PPi/Pi ratio is highly important in the second step of mineralization, where the initial hydroxyapatite (released from matrix vesicles) aggregates and expands in the extracellular matrix.[41] The plasma levels of ionized calcium and phosphate were comparable between groups. To note, the normal ATx rats had slightly lower phosphate levels compared with the other two groups; however, the levels were still within normal range.

Four weeks with a calcified aorta graft resulted in less osteoid and a tendency to fewer mature osteoblasts. Gene analysis also showed downregulation of osteocalcin and upregulation of

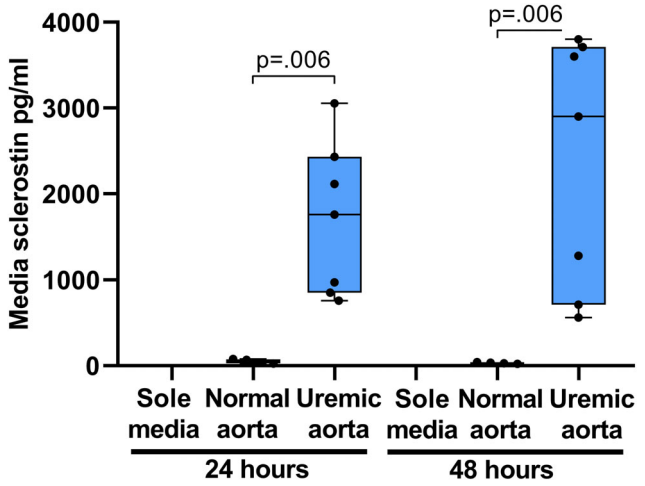

Fig 7. Aorta rings (1 mm) from normal rats ($n = 2$) and uremic rats ($n = 3$) were incubated for 24 or 48 hours (8 rings/well). The media's concentration of sclerostin was measured by ELISA. The media from the incubation of uremic calcified aorta rings had a very high concentration of sclerostin, clearly demonstrating a high secretion of sclerostin from the calcified aorta rings. Media samples from normal rats $n = 4$, 24 hours and $n = 4$, 48 hours, and from uremic rats $n = 7$, 24 hours and $n = 7$, 48 hours.

collagen I; this may indicate a shift toward early stage of osteoblast differentiation. We could not yet detect a difference in trabecular thickness or numbers by μCT and bone histomorphometry after 4 weeks of aorta implantation. The follow-up period of 4 weeks may not be optimal to detect the changes reflected in the gene expression analysis. Also, similar bone formation rate was found in the three groups, which to an important extent must be ascribed to the significant biological variation inherent to this parameter in rats with normal renal function.

RANKL was downregulated in uremic ATx rats, indicating an uncoupled osteoblast/osteocyte–osteoclast signaling, namely the stimulation of osteoclast differentiation and activation. However, bone resorption as indicated histomorphometrically by the erodic surface did not differ between the three groups, although a nonsignificant trend toward a higher number of osteoclasts was found in the uremic ATx rats. In line herewith, an upregulation of cathepsin K was found in the gene analysis. Combining all the analyses of the bone, the overall picture points toward an effect on bone formation and mineralization as well as resorption. In addition, the balance between Wnt and BMP signaling in bone was also shifted in the uremic ATx rats, as illustrated by upregulation of sclerostin and downregulation of BMP2. Even though we cannot demonstrate the direct link to inhibition of the Wnt pathway, these results are in accordance to what would be reasonably be expected if this pathway was hindered.[47] All in all, our data point toward an effect of VC on bone turnover in general.

We measured plasma levels of PTH and FGF23 as well as bone FGF23 mRNA and found no difference between the three groups under study, indicating that these hormones are not directly involved in VC to bone signaling. Sclerostin binds the co-receptor Lrp5/6 and thereby inhibits canonical Wnt signaling.[35] Our group and others suggested that sclerostin could be the signaling molecule in the VC-bone axis because it is highly expressed in calcified vessels and as such could potentially be secreted into circulation.[24,39,48] Our model of CKD-induced VC was accompanied by a large increase in plasma sclerostin, which was not reflected in the uremic rat's bone's expression of sclerostin as its mRNA levels were significantly lower to normal controls. The ex vivo cultures of aorta demonstrated a high secretion of sclerostin from the calcified aorta. To examine if the calcified graft increased the plasma levels of sclerostin, we measured plasma sclerostin in all rats 4 weeks after aorta transplantation and found similar levels. On the contrary, De Maré and colleagues found a gradual increase in plasma sclerostin as VC progressed. However, the absence of an increased bone expression of sclerostin similar to our VC model points to an extraskeletal sclerostin production.[39] Whereas the warfarin model results in generalized VC in the cardiovascular system, calcification in our transplant model is restricted to the abdominal aorta graft. Therefore, it may be difficult to detect the possible secretion of sclerostin from the calcified graft. Furthermore, detection of early or temporary changes in plasma sclerostin levels was not included in the present protocol. In our study, we found an upregulation of bone sclerostin mRNA in uremic ATx rats, which was not reflected in the plasma levels of sclerostin. The discrepancy between bone mRNA levels and plasma levels of sclerostin is not clear. Normal kidney function was found in the present study as in the study of De Maré and colleagues.

Another potential signaling molecule from the uremic calcified graft could be SFRP4, a decoy receptor for Wnt ligand. SFRP4 antagonizes both canonical and non-canonical Wnt signaling in bone.[49] Because of limitation of plasma volume in the rat, we did not measure plasma SFRP4 in the present study. The other known SFRPs are not upregulated in our VC model. Others have proposed a role of the Wnt inhibitor Dickkopf-1 (Dkk1) in the progression of the bone disorder and VC in kidney disease.[50] Nevertheless, Dkk1 is not upregulated in the calcified vasculature in our model as well as Dkk2 and Dkk4. Recently, the member of the transforming growth factor-β (TGF-β) family Activin A has been proposed to play a role in the CKD-MBD and it is linked to TGF- β and Wnt signaling.[51] Activin A is induced in kidney disease along with a rise in its plasma levels. An increase in systemic Activin A is also found in aging, osteoporosis, and diabetes.[37,52] In our RNAseq study, we found a significant upregulation of *Inhba* coding for Activin A in the calcified aorta, but plasma levels of Activin A were not measured in the present study. Still, Activin A is believed to induce bone loss, as signaling through the Activin receptor type 2a in bone primarily stimulates osteoclastogenesis and bone resorption.[53]

We found increased β-catenin mRNA levels compared with the control groups, indicating changes in the canonical Wnt/β-catenin signaling pathway. Even though the mRNA levels of β-catenin were increased, this does not directly imply increased Wnt/β-catenin signaling because the protein is highly regulated post-transcriptionally by the phosphorylated/non-phosphorylated state. β-catenin is continuously being expressed in the cell. In the absence of Wnt activation, the protein complex consisting of adenomatous polyposis coli (APC), axin, and glycogen synthase kinase 3 (GSK3) bind and phosphorylate β-catenin, resulting in rapid degradation.[54] Phosphorylated/total β-catenin protein was not measured in the present study. In a previous study from our group, normal DA rats were treated with the canonical Wnt/β-catenin signal pathway inhibitor ICG-001.[55] In accordance with results of the present study, gene analysis by qPCR of these ICG-001-treated rats showed a similar

pattern with upregulation of β-catenin mRNA levels in bone, indicating that inhibition of the canonical Wnt/β-catenin signal pathway in DA rats induces increased β-catenin mRNA levels.[55] Wnt target genes c-Myc and Axin2 were significantly downregulated in uremic ATx, supporting that Wnt pathway is affected in bone. The expression of Cyclin D1 was, however, not different between the groups. It is well demonstrated that activation of the canonical Wnt/β-catenin results in bone formation; however, the downstream signaling pathways are largely unknown.[36]

We found increased mRNA bone expression of Snail1 in the study. This transcription factor plays a key role in epithelial to mesenchymal transition in physiology and pathophysiology. However, pleiotropic functions of the protein are being identified.[56] Several regulators of its expression have been found, including both canonical and non-canonical TGFβ/SMAD and Wnt signaling.[57] In bone, Snail1 is expressed by the osteoblast and it is necessary for the early steps of differentiation in the cell. However, Snail1 must be downregulated for late osteoblast differentiation and mineralization and so overexpression of Snail1 results in impaired bone formation and mineralization.[58] The increase in Snail1 expression may have affected osteoblastogenesis in our study. Similar to our results, increased Snail1 activity results in downregulation of RANKL, osteocalcin, and upregulation of collagen I.[58] Still, it is a challenge to identify the initial effect on bone turnover and its consequences, as bone cells and processes in the remodeling cycle are all interconnected. We propose that sclerostin is secreted by the calcified aorta graft and inhibits Wnt pathway in bone. Thus all the present results may illustrate complemental processes in a complex dynamic biological system.

In conclusion, calcified vasculature secretes the Wnt inhibitor sclerostin. The presence of VC alters bone metabolism along with significant changes in several pathways in bone. On the basis of our results, we propose the existence of a vasculature to bone tissue cross-talk. We speculate that a pathological cross-talk between VC and bone tissues generates a negative spiral of demineralization of bone and mineralization of the vasculature.

Disclosures

All authors state that they have no conflicts of interest.

Acknowledgments

We thank our very skilled lab technicians Kirsten Bang and Nina Sejthen for their excellent work. The study was supported by the Danish Heart Association (grant 19-R132-A9209-22141 and 16-R107-A6720-22012 to MLM), Augustinus Foundation (grant 19-2370 to MLM), and the Kirsten and Freddie Johansen Foundation (grant to KO).

Author Contributions: Maria Mace: Conceptualization; data curation; formal analysis; funding acquisition; investigation; methodology; project administration; visualization; writing-original draft; writing-review and editing. Eva Gravesen: Investigation; project administration. Anders Nordholm: Investigation. Soeren Egstrand: Investigation. Marya Morevati: Investigation. Carsten Nielsen: Investigation; software. Andreas Kjaer: Investigation; software. Geert Behets: Formal analysis; investigation; visualization. Patrick D'Haese: Formal analysis; investigation; visualization; writing-review and editing. Klaus Olgaard: Conceptualization; formal analysis; funding acquisition; investigation; methodology; supervision; writing-review and editing. Ewa Lewin: Conceptualization; formal analysis; funding acquisition; investigation; methodology; supervision; writing-review and editing.

Peer Review

The peer review history for this article is available at https://publons.com/publon/10.1002/jbmr.4203.

References

1. Hyder JA, Allison MA, Criqui MH, Wright CM. Association between systemic calcified atherosclerosis and bone density. Calcif Tissue Int. 2007;80(5):301–6.
2. Edmonds ME. Medial arterial calcification and diabetes mellitus. Z Kardiol. 2000;89(Suppl 2):101–4.
3. Toussaint ND, Lau KK, Strauss BJ, Polkinghorne KR, Kerr PG. Associations between vascular calcification, arterial stiffness and bone mineral density in chronic kidney disease. Nephrol Dial Transplant. 2008;23(2):586–93.
4. Raggi P, Bellasi A, Ferramosca E, Block GA, Muntner P. Pulse wave velocity is inversely related to vertebral bone density in hemodialysis patients. Hypertension. 2007;49(6):1278–84.
5. Hak AE, Pols HA, van Hemert AM, Hofman A, Witteman JC. Progression of aortic calcification is associated with metacarpal bone loss during menopause: a population-based longitudinal study. Arterioscler Thromb Vasc Biol. 2000;20(8):1926–31.
6. Laroche M, Delmotte A. Increased arterial calcification in Paget's disease of bone. Calcif Tissue Int. 2005;77(3):129–33.
7. Schulz E, Arfai K, Liu X, Sayre J, Gilsanz V. Aortic calcification and the risk of osteoporosis and fractures. J Clin Endocrinol Metab. 2004;89(9):4246–53.
8. Kiel DP, Kauppila LI, Cupples LA, Hannan MT, O'Donnell CJ, Wilson PW. Bone loss and the progression of abdominal aortic calcification over a 25 year period: the Framingham Heart Study. Calcif Tissue Int. 2001;68(5):271–6.
9. Naves M, Rodriguez-Garcia M, Diaz-Lopez JB, Gomez-Alonso C, Cannata-Andia JB. Progression of vascular calcifications is associated with greater bone loss and increased bone fractures. Osteoporos Int. 2008;19(8):1161–6.
10. Tanko LB, Christiansen C, Cox DA, Geiger MJ, McNabb MA, Cummings SR. Relationship between osteoporosis and cardiovascular disease in postmenopausal women. J Bone Miner Res. 2005;20(11):1912–20.
11. Kado DM, Browner WS, Blackwell T, Gore R, Cummings SR. Rate of bone loss is associated with mortality in older women: a prospective study. J Bone Miner Res. 2000;15(10):1974–80.
12. Lewis JR, Eggermont CJ, Schousboe JT, et al. Association between abdominal aortic calcification, bone mineral density, and fracture in older women. J Bone Miner Res. 2019;34(11):2052–60.
13. Persy V, D'Haese P. Vascular calcification and bone disease: the calcification paradox. Trends Mol Med. 2009;15(9):405–16.
14. Moe S, Drueke T, Cunningham J, et al. Definition, evaluation, and classification of renal osteodystrophy: a position statement from Kidney Disease: Improving Global Outcomes (KDIGO). Kidney Int. 2006;69(11):1945–53.
15. Foley RN, Parfrey PS, Sarnak MJ. Epidemiology of cardiovascular disease in chronic renal disease. J Am Soc Nephrol. 1998;9(12 Suppl):S16–23.
16. Hruska KA, Seifert M, Sugatani T. Pathophysiology of the chronic kidney disease-mineral bone disorder. Curr Opin Nephrol Hypertens. 2015;24(4):303–9.
17. Lewin E, Olgaard K. The vascular secret of klotho. Kidney Int. 2015;87(6):1089–91.
18. Mace ML, Gravesen E, Hofman-Bang J, Olgaard K, Lewin E. Key role of the kidney in the regulation of fibroblast growth factor 23. Kidney Int. 2015;88(6):1304–13.

19. Nordholm A, Mace ML, Gravesen E, Olgaard K, Lewin E. A potential kidney-bone axis involved in the rapid minute-to-minute regulation of plasma Ca2+. BMC Nephrol. 2015;16:29.
20. Elias RM, Dalboni MA, Coelho ACE, Moyses RMA. CKD-MBD: from the pathogenesis to the identification and development of potential novel therapeutic targets. Curr Osteoporos Rep. 2018;16(6):693–702.
21. Sarnak MJ, Levey AS, Schoolwerth AC, et al. Kidney disease as a risk factor for development of cardiovascular disease: a statement from the American Heart Association councils on kidney in cardiovascular disease, high blood pressure research, clinical cardiology, and epidemiology and prevention. Circulation. 2003;108(17):2154–69.
22. Durham AL, Speer MY, Scatena M, Giachelli CM, Shanahan CM. Role of smooth muscle cells in vascular calcification: implications in atherosclerosis and arterial stiffness. Cardiovasc Res. 2018;114(4): 590–600.
23. Neven E, De Schutter TM, De Broe ME, D'Haese PC. Cell biological and physicochemical aspects of arterial calcification. Kidney Int. 2011;79 (11):1166–77.
24. Rukov JL, Gravesen E, Mace ML, et al. Effect of chronic uremia on the transcriptional profile of the calcified aorta analysed by RNA-sequencing. Am J Physiol Renal Physiol. 2016;310(6):F477–91.
25. Lewin E, Wang W, Olgaard K. Reversibility of experimental secondary hyperparathyroidism. Kidney Int. 1997;52(5):1232–41.
26. Lewin E, Garfia B, Recio FL, Rodriguez M, Olgaard K. Persistent down-regulation of calcium-sensing receptor mRNA in rat parathyroids when severe secondary hyperparathyroidism is reversed by an isogenic kidney transplantation. J Am Soc Nephrol. 2002;13(8):2110–6.
27. Lewin E, Colstrup H, Pless V, Ladefoged J, Olgaard K. A model of reversible uremia employing isogenic kidney transplantation in the rat. Reversibility of secondary hyperparathyroidism. Scand J Urol Nephrol. 1993;27(1):115–20.
28. Hofman-Bang J, Martuseviciene G, Santini MA, Olgaard K, Lewin E. Increased parathyroid expression of klotho in uremic rats. Kidney Int. 2010;78(11):1119–27.
29. Huan J, Olgaard K, Nielsen LB, Lewin E. Parathyroid hormone 7-84 induces hypocalcemia and inhibits the parathyroid hormone 1-84 secretory response to hypocalcemia in rats with intact parathyroid glands. J Am Soc Nephrol. 2006;17(7):1923–30.
30. Vandesompele J, De Preter K, Pattyn F, et al. Accurate normalization of real-time quantitative RT-PCR data by geometric averaging of multiple internal control genes. Genome Biol. 2002;3(7):1–11.
31. Parfitt AM, Drezner MK, Glorieux FH, et al. Bone histomorphometry: standardization of nomenclature, symbols, and units. Report of the ASBMR Histomorphometry Nomenclature Committee. J Bone Miner Res. 1987;2(6):595–610.
32. Behets GJ, Spasovski G, Sterling LR, et al. Bone histomorphometry before and after long-term treatment with cinacalcet in dialysis patients with secondary hyperparathyroidism. Kidney Int. 2015;87 (4):846–56.
33. Dempster DW, Compston JE, Drezner MK, et al. Standardized nomenclature, symbols, and units for bone histomorphometry: a 2012 update of the report of the ASBMR Histomorphometry Nomenclature Committee. J Bone Miner Res. 2013;28(1):2–17.
34. Gravesen E, Lerche Mace M, Nordholm A, et al. Exogenous BMP7 in aortae of rats with chronic uremia ameliorates expression of profibrotic genes, but does not reverse established vascular calcification. PLoS One. 2018;13(1):e0190820.
35. Li X, Zhang Y, Kang H, et al. Sclerostin binds to LRP5/6 and antagonizes canonical Wnt signaling. J Biol Chem. 2005;280(20):19883–7.
36. Houschyar KS, Tapking C, Borrelli MR, et al. Wnt pathway in bone repair and regeneration—what do we know so far. Front Cell Dev Biol. 2018;6:170.
37. Nordholm A, Mace ML, Gravesen E, et al. Klotho and activin a in kidney injury: plasma klotho is maintained in unilateral obstruction despite no upregulation of klotho biosynthesis in the contralateral kidney. Am J Physiol Renal Physiol. 2018;314(5):F753–F62.
38. Frye MA, Melton LJ III, Bryant SC, et al. Osteoporosis and calcification of the aorta. Bone Miner. 1992;19(2):185–94.
39. De Mare A, Maudsley S, Azmi A, et al. Sclerostin as regulatory molecule in vascular media calcification and the bone-vascular Axis. Toxins. 2019;11(7).
40. Lomashvili KA, Narisawa S, Millan JL, O'Neill WC. Vascular calcification is dependent on plasma levels of pyrophosphate. Kidney Int. 2014;85 (6):1351–6.
41. Orimo H. The mechanism of mineralization and the role of alkaline phosphatase in health and disease. J Nippon Med Sch. 2010;77 (1):4–12.
42. Singh K, Deonarine D, Shanmugam V, et al. Calcium-binding properties of osteopontin derived from non-osteogenic sources. J Biochem. 1993;114(5):702–7.
43. Icer MA, Gezmen-Karadag M. The multiple functions and mechanisms of osteopontin. Clin Biochem. 2018;59:17–24.
44. Saki F, Sheikhi A, Omrani GHR, Karimi H, Dabbaghmanesh MH, Mousavinasab SN. Evaluation of bone mineral density in children with type I diabetes mellitus and relationship to serum levels of osteopontin. Drug Res. 2017;67(9):527–33.
45. Wei QS, Huang L, Tan X, Chen ZQ, Chen SM, Deng WM. Serum osteopontin levels in relation to bone mineral density and bone turnover markers in postmenopausal women. Scand J Clin Lab Invest. 2016; 76(1):33–9.
46. Addison WN, Azari F, Sorensen ES, Kaartinen MT, McKee MD. Pyrophosphate inhibits mineralization of osteoblast cultures by binding to mineral, up-regulating osteopontin, and inhibiting alkaline phosphatase activity. J Biol Chem. 2007;282(21):15872–83.
47. Krishnan V, Bryant HU, Macdougald OA. Regulation of bone mass by Wnt signaling. J Clin Invest. 2006;116(5):1202–9.
48. Evenepoel P, Opdebeeck B, David K, D'Haese PC. Bone-vascular Axis in chronic kidney disease. Adv Chronic Kidney Dis. 2019;26(6): 472–83.
49. Nakanishi R, Shimizu M, Mori M, et al. Secreted frizzled-related protein 4 is a negative regulator of peak BMD in SAMP6 mice. J Bone Miner Res. 2006;21(11):1713–21.
50. Fang Y, Ginsberg C, Seifert M, et al. CKD-induced wingless/integration1 inhibitors and phosphorus cause the CKD-mineral and bone disorder. J Am Soc Nephrol. 2014;25(8):1760–73.
51. Hruska KA, Sugatani T, Agapova O, Fang Y. The chronic kidney disease—mineral bone disorder (CKD-MBD): advances in pathophysiology. Bone. 2017;100:80–6.
52. Nordholm A, Egstrand S, Gravesen E, et al. Circadian rhythm of activin A and related parameters of mineral metabolism in normal and uremic rats. Pflugers Arch. 2019;471(8):1079–94.
53. Sugatani T, Agapova OA, Fang Y, et al. Ligand trap of the activin receptor type IIA inhibits osteoclast stimulation of bone remodeling in diabetic mice with chronic kidney disease. Kidney Int. 2017;91(1): 86–95.
54. Baron R, Kneissel M. WNT signaling in bone homeostasis and disease: from human mutations to treatments. Nat Med. 2013;19(2):179–92.
55. Gravesen E, Nordholm A, Mace M, et al. Effect of inhibition of CBP-coactivated beta-catenin-mediated Wnt signalling in uremic rats with vascular calcifications. PLoS One. 2018;13(8):e0201936.
56. Wu Y, Zhou BP. Snail: more than EMT. Cell Adh Migr. 2010;4(2): 199–203.
57. Simon-Tillaux N, Hertig A. Snail and kidney fibrosis. Nephrol Dial Transplant. 2017;32(2):224–33.
58. de Frutos CA, Dacquin R, Vega S, Jurdic P, Machuca-Gayet I, Nieto MA. Snail1 controls bone mass by regulating Runx2 and VDR expression during osteoblast differentiation. EMBO J. 2009;28(6):686–96.